Terahertz Detection by High Electron Mobility Transistor: Effect of Drain Current

J.-Q. Lu and M.S. Shur

Center for Integrated Electronics and Electronics Manufacturing,
Rensselaer Polytechnic Institute, Troy, New York 12180
Tel: (518) 276-2201, luj@rpi.edu, shurm@rpi.edu

Abstract

We report on a new regime of operation of High Electron Mobility Transistor (HEMT) terahertz detectors, in which we apply a constant (*dc*) drain bias. The measured responsivity increases with the drain current by more than an order of magnitude and saturates at the *dc* bias corresponding to the saturation of the *dc* drain current for given gate voltage. We link this increase in the detector responsivity to the drain bias dependence of the gate-to-source and gate-to-drain capacitances, which results in a much greater asymmetry in the boundary conditions for plasma waves. These results confirm our model linking the HEMT detector response to the propagation of overdamped plasma waves in the device channel.

Introduction

Plasma waves in short-channel High Electron Mobility Transistors (HEMTs) have a resonant response at terahertz frequencies [1]. The HEMTs operating in a plasma wave regime should respond at much higher frequencies than conventional, transit-time limited devices, since the plasma waves propagate much faster than electrons. We refer to such devices as *plasma wave electronics* devices. The rectification of the plasma waves (linked to the asymmetry of the boundary conditions at the source and the drain) can be used for the tunable detection of electromagnetic radiation at terahertz frequencies.

This plasma wave electronics short-channel HEMT detector produces an open circuit *dc* voltage, which is proportional to the intensity of the incoming terahertz radiation with a resonance response to electromagnetic radiation at the plasma oscillation frequency. The resonant plasma frequency can be tuned by the gate bias, which makes the plasma wave electronics detector suitable for many applications involving far infrared spectroscopy for the detection of chemical and biological substances. The dynamic range of such a detector is limited by the gate voltage swing, since the responsivity decreases when the terahertz radiation induced *ac* voltage becomes on the order of a few percent of gate voltage swing.

Longer HEMTs exhibit a non-resonant, broadband response to electromagnetic

radiation caused by overdamped plasma waves that degenerate into space charge waves in very long devices. Such devices can still be used as broadband detectors for frequencies up to several tens of terahertz.

Our recent experimental data (see [2,3]) confirm many features of the theoretical predictions but also pose many questions. We have demonstrated non-resonant detectors fabricated using AlGaAs/GaAs [4] and AlGaN/GaN HFETs [5] operating at frequencies below 20 GHz. More recently, we have reported on the implementation of the AlGaAs/GaAs terahertz HEMT detector [3,6], where the devices operated at 2.5 THz, which is about 30 times higher than the transistor cutoff frequency.

In this paper, we report on a new regime of operation of such HEMT terahertz detectors that allowed us to increase the device responsivity by more than an order of magnitude. The motivation for this new regime comes from our theoretical analysis of the effect of the boundary conditions [5,7], which shows that the maximum detector response occurs when the asymmetry between the boundary conditions at the source and drain contacts of the device is the largest. (For a completely symmetrical structure with symmetrical boundary conditions, we, of course, expect and predict a zero detector response.)

Experimental Results

Device Characterizations

The experimental results reported in this paper were obtained using a GaAs/AlGaAs low noise HEMT chip (Fujitsu FHR20X) [8]. Figures 1 through 4 show the measured device characteristics. The estimated threshold voltage for this device V_T = -0.6 V. The device gate width was W = 100 μm (two section of 50 μm each). The estimated gate length was approximately L = 0.15 μm.

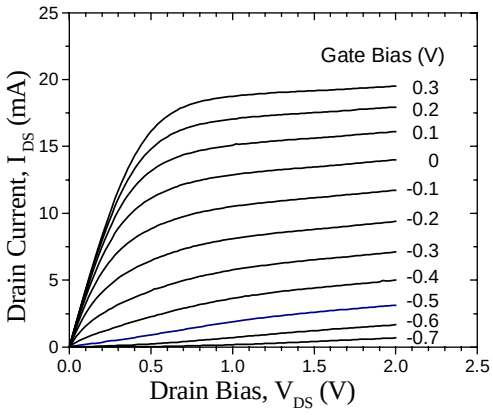

Fig. 1. I-V characteristics of the HEMT. The data was taken when only left source is grounded and the right source is floating.

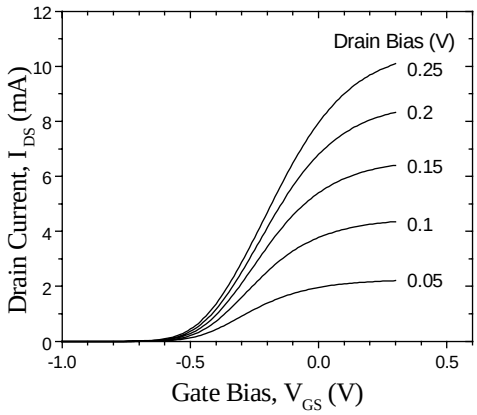

Fig. 2. HEMT transfer characteristics. The data was taken when only left source is grounded and the right source is floating.

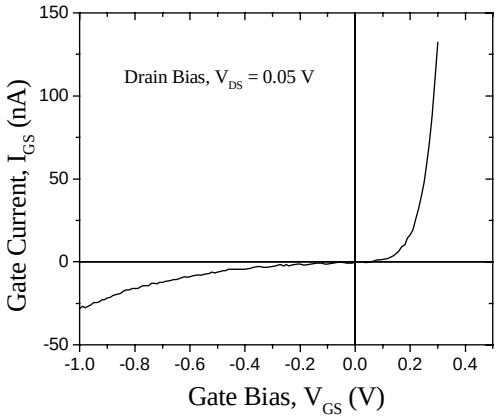

Fig. 3. HEMT FHR20X gate leakage current versus gate bias. The drain source bias is 0.05 V.

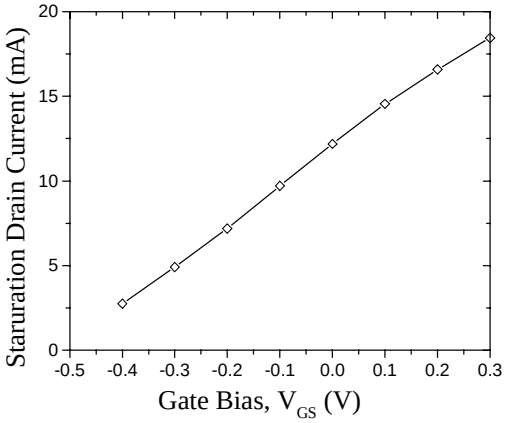

Fig. 4. Saturation drain current vs. gate bias, Isat vs V_{GS}. The data are extracted from the device I-V characteristics shown in Fig. 1.

Figure 5 shows the gain versus frequency of the HEMT, calculated from the scattering parameters taken from the Fujitsu Databook [8], where the bias condition is as follows: V_{DS} = 2 V, I_{DS} = 5 mA.

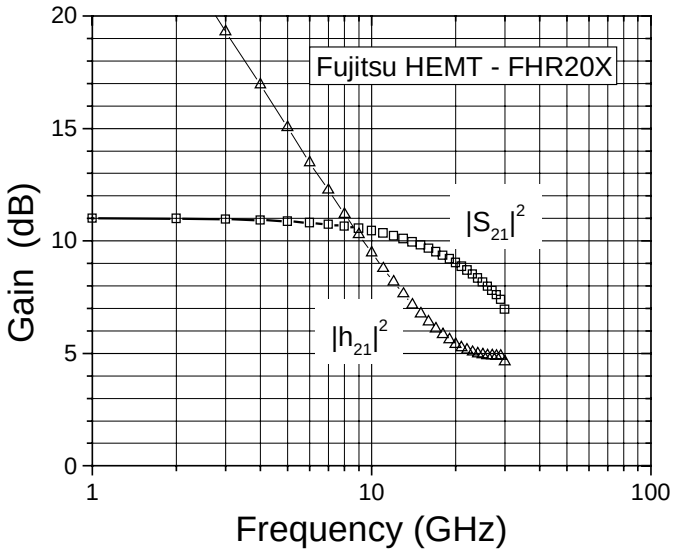

Fig. 5. The gain versus frequency of the HEMT.

Both the device operating frequency (~18 GHz) and the cutoff frequency are orders of magnitude smaller than the terahertz frequency of the radiation used in our experiments. This makes it difficult to use lumped equivalent circuit for the interpretation of our experiments, even though we believe that the asymmetry in the values of the gate-to-source and gate-to-drain capacitances still represent a crude measure of the boundary conditions for the terahertz signal (see our discussion below).

Terahertz Detection

The terahertz detector was fabricated using a Fujitsu FHR20X HEMT mounted on a quartz substrate. The device threshold voltage is close to V_T = -0.6 V, extracted from the measured device *dc* characteristics. A CO_2-pumped far-infrared gas laser served as a source of 2.5 THz radiation. The polarized laser beam was chopped and focused on the sample as shown in Fig. 6. The induced *dc* drain voltage, U_{DS} (that appeared in response to the THz radiation), was superimposed on the drain bias voltage (causing a *dc* drain current, I_{DS}). U_{DS} was measured using lock-in technique. The detector was tuned by a *dc* gate bias, V_{GS}, and the response was a strong function of I_{DS}.

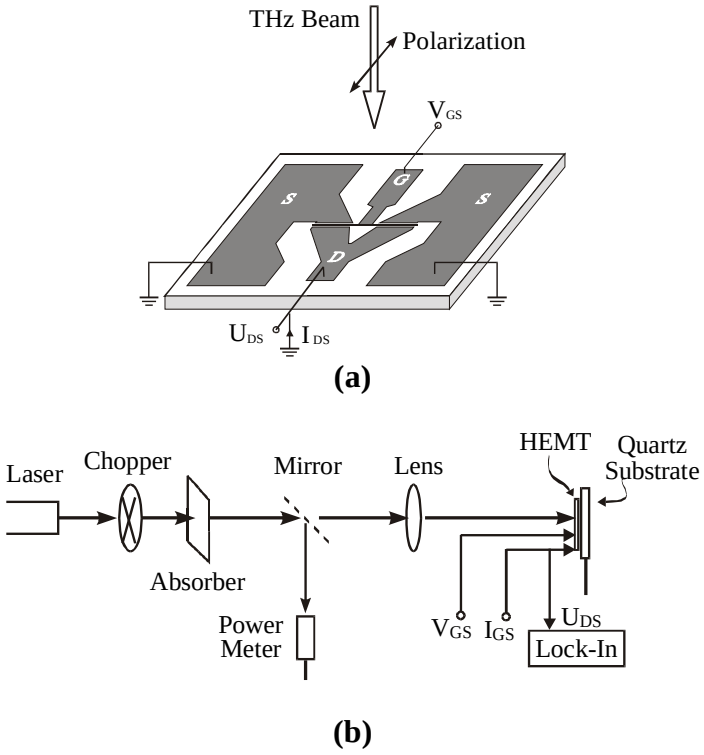

Fig. 6. Detector layout using a Fujitsu FHR20X HEMT with V_T = -0.6 V, and (b) measurement setup with a 2.5 THz laser. The detector response - the *dc* drain voltage, U_{DS}, was measured using lock-in technique.

In the new regime of operation, we apply a *dc* drain bias. The drain bias dependence of the gate-to-source and gate-to-drain capacitances leads to a much greater asymmetry in the boundary conditions for plasma waves and greatly enhances the detector responsivity. As can be seen in Fig. 7, the detector response, *dc* drain voltage, U_{DS}, increases significantly with the applied *dc* drain current, compared with the response without drain current (see the inset of Fig. 7).

We should also notice sharp spikes in the response at the gate bias near the threshold for drain currents from 0.1 to 0.5 μA. These spikes were quite reproducible. However, at the moment we have no explanation for these peaks.

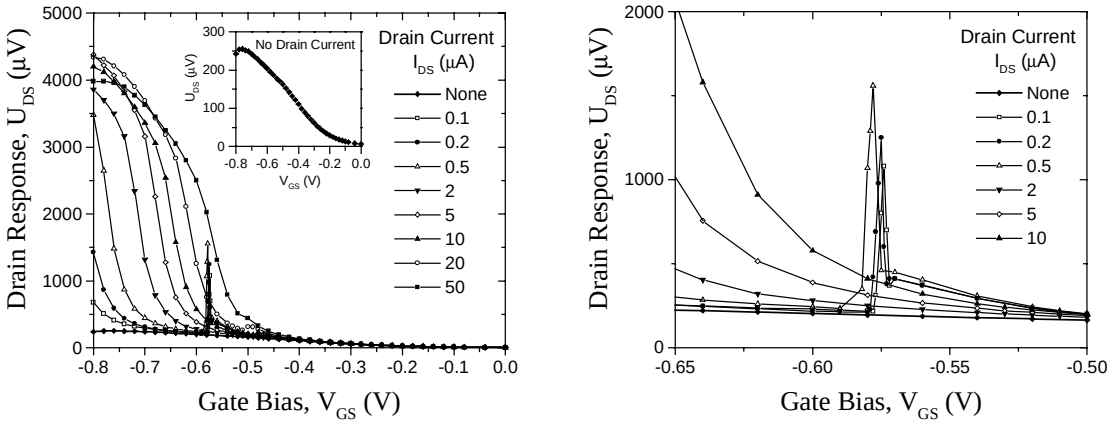

Fig. 7. Measured detector responses (U_{DS}) versus gate bias (V_{GS}) at different *dc* drain currents (I_{DS}). Inset is the drain response without a *dc* drain current. Also shown the measured spikes in response in an expanded scale (left figure).

We also notice that the response peaks at the gate bias somewhat below threshold (see Fig. 8). This is predicted by our theory that links the reduction in the response at the gate bias well below threshold due to the gate leakage current [9].

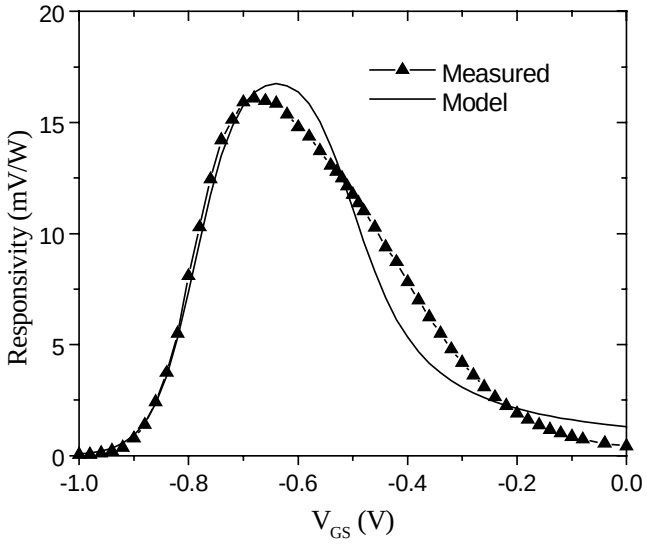

Fig. 8. Typical detector responsivity as a function of gate bias. The solid line is a first order simulation using a HEMT detector model, which is good also for the subthreshold regime [9]. The parameters used for the simulation are threshold voltage, V_T = -0.52 V, ideality factor extracted from Fig. 2, η = 1.5, and the leakage factor, $\Gamma = 10^{-3}$.

Fig. 9 shows detector response versus the drain current at different gate bias. The response increases with the applied *dc* drain current and saturates at a saturation drain current for given gate bias.

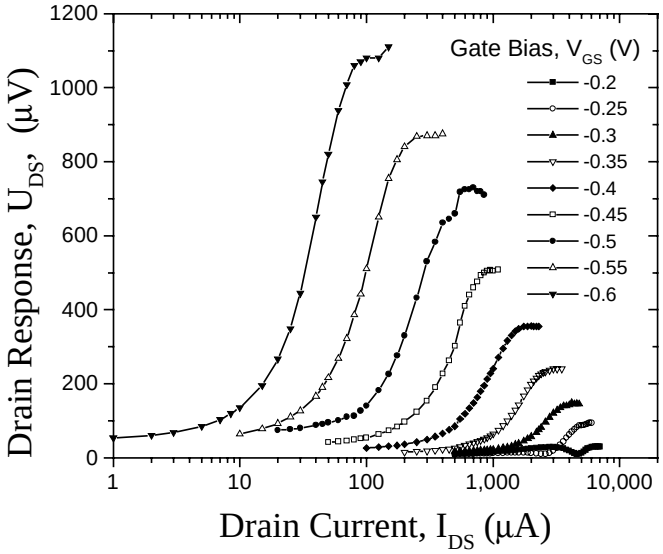

Fig. 9. Measured detector responses (U_{DS}) versus *dc* drain current (I_{DS}) at different gate biases (V_{GS}) at 2.5 THz.

Fig. 10 shows the gate bias dependence of the saturation currents extracted from I-V characterization and from Fig. 9, U_{DS} versus I_{DS} curve. These results confirm our model linking the responsivity increase to the drain bias dependence of the HEMT capacitances.

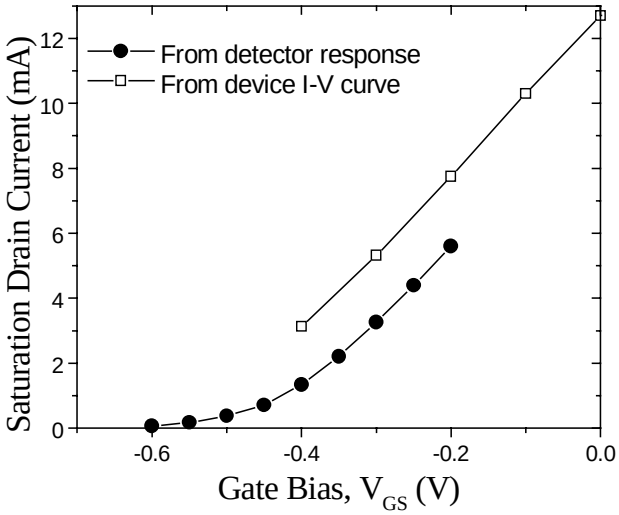

Fig. 10. The saturation drain currents versus gate bias. The circle data are extracted from Fig. 9, U_{DS} versus I_{DS} curve. The square data are extracted from the device I-V characteristics in Fig. 1, where the drain current saturates at certain drain bias for a given gate bias.

Discussion

Fig. 11 shows the calculated dependencies of the gate-to-source and gate-to-drain capacitances for zero and -0.3 V gate bias for an AlGaAs/GaAs HEMT with parameters corresponding to our devices. The gate-to-source and gate-to-drain capacitance values, C_{GS} and C_{GD}, are given as [10]:

$$C_{GS} = \frac{2}{3} C_{ch} \left[1 - \left(\frac{V_{GT} - V_{DSe}}{2V_{GT} - V_{DSe}} \right)^2 \right],$$

$$C_{GS} = \frac{2}{3} C_{ch} \left[1 - \left(\frac{V_{GT}}{2V_{GT} - V_{DSe}} \right)^2 \right],$$

where C_{ch} is gate channel capacitance of the HEMT at zero drain-source bias, the gate bias swing $V_{GT} = V_{GS}-V_T$, and V_{DSe} is the effective intrinsic drain-source voltage given by:

$$V_{DSe} = \frac{1}{2} \left[V_{DS} + V_{GTe} - \sqrt{V_d^2 + (V_{DS} - V_{GTe})^2} \right].$$

Here, V_d is a constant voltage that determines the width of the transition region and V_{GTe} is an effective gate voltage overdrive (equal to V_{GT} above threshold and of the order of thermal voltage in the subthreshold regime). The details of the capacitance model are described in Reference [10].

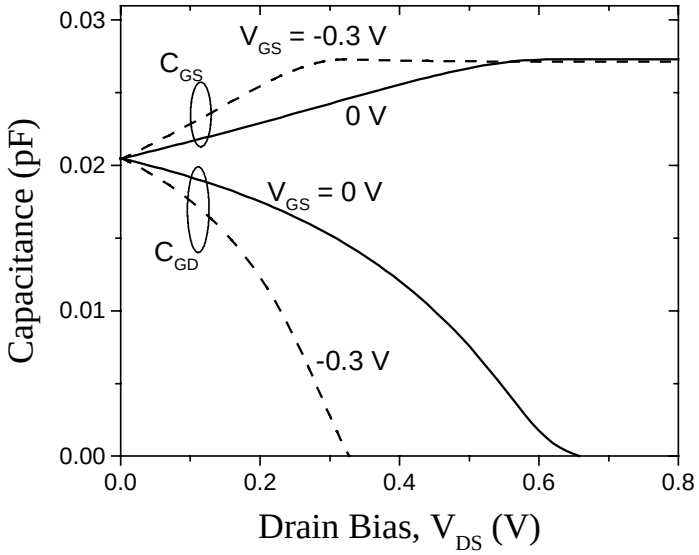

Fig. 11. Gate-to-source and gate-to-drain capacitances for zero and -0.3 gate biases: C_{GS} and C_{GD} versus drain bias. Parameters used in the calculation: threshold voltage, V_T = -0.6 V, gate width and length W = 50

μm and L = 0.15 μm, respectively, AlGaAs thickness, d_i = 25 nm, maximum density of the two-dimensional (2D) electron gas, n_{smax} = $2.5x10^{16}m^{-2}$.

As can be seen from the Fig. 11, at the saturation voltage, which is approximately 0.6 V in the frame of this model for V_{GS} = 0 (0.3 V for V_{GS} = -0.3 V), C_{GD} is nearly zero, whereas C_{GS} reaches its maximum value. Hence, the drain bias dependence of the gate-to-source and gate-to-drain capacitances leads to a much greater asymmetry in the boundary conditions for plasma waves and greatly enhances the detector responsivity. This asymmetry reaches its maximum at smaller drain biases for smaller (larger negative) gate biases (compare the curves for V_{GS} = -0.3 V and V_{GS} = 0 V).

Figure 12 shows that the response saturates as a function of the drain bias at approximately the *dc* drain saturation voltage of I-V characteristics. This is in agreement with our data shown in Fig. 10 and with our interpretation linking this behavior to the enhanced asymmetry in the boundary conditions (see Fig. 11).

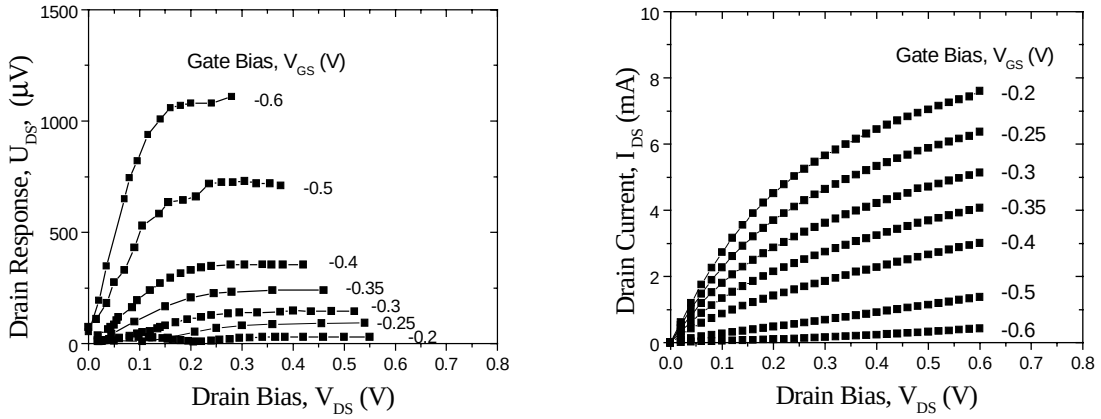

(a) **(b)**

Fig. 12. Comparison of the drain response versus drain bias to *dc* drain current versus drain bias. (a) The drain response versus drain bias curve was converted from Fig. 9. (b) The I-V characteristics are part of Fig. 1.

Conclusions

Our experimental data support the plasma wave mechanism of the terahertz detection by High Electron Mobility Transistors. These results confirm that the gate leakage current does not play a role in the terahertz detection in the above threshold regime, since this current decreases with the drain bias. A strong enhancement of the detector responsivity by a constant drain current and the saturation of this response when the *dc* drain current reaches saturation point confirm the dominant role of the asymmetry in the boundary conditions in determining the detector responsivity.

Acknowledgments

This work has been supported by DARPA (Program Manager, Dr. Edgar Martinez) and by ARO (Program Manager, Dr. Dwight Woolard). We are also grateful to Dr. J. Hesler and Mr. L. Suddarth of University of Virginia for their help with the measurements and to Professor M. Dyakonov for useful discussions.

References:

[1] M. Dyakonov and M. S. Shur, "Detection, mixing, and frequency multiplication of terahertz radiation by two dimensional electronic fluid", *IEEE Trans. Electron Dev.*, vol. 43, no. 3, pp. 380-387, 1996.

[2] M.S. Shur, J.-Q. Lü, and M. Dyakonov, "Plasma Wave Electronics: Terahertz Sources and Detectors Using Two Dimensional Electronic Fluid in High Electron Mobility Transistors", *Proceedings of 1998 IEEE 6th International Conference on Terahertz Electronics*, Leads, UK, pp. 127-130, 1998

[3] J.-Q. Lü, M. S. Shur, J. L. Hesler, L. Sun, and R. Weikle II, "A Resonant Terahertz Detector Utilizing a High Electron Mobility Transistor", *IEDM Technical Digest*, pp. 453-456, San Francisco, CA, 1998

[4] R. Weikle, J.-Q. Lü, M. S. Shur, M. I. Dyakonov, *Electronics Letters*, vol. 32, no. 23, pp. 2148-2149, 1996

[5] J.-Q. Lü, M. S. Shur, R. Weikle, M. I. Dyakonov, and M. A. Khan, *Proceedings of 16th Conference on Advanced Concepts in High Speed Semiconductor Devices and Circuits*, Ithaca, NY, pp. 211-217, 1997

[6] J.-Q. Lü, M. S. Shur, J. L. Hesler, L. Sun, and R. Weikle, *IEEE Electron Dev. Lett*., vol. 19, No. 10, pp. 373-375, 1998

[7] J.-Q. Lu and M.S. Shur, "Effect of Loading on Plasma Wave Detector Utilizing Two-Dimensional Electron Fluid", http://www.rpi.edu/~luj/loadeffect.htm, Dec. 2000.

[8] Fujitsu Microwave Semiconductor Databook (1999), Fujitsu Compound Semiconductor, Inc., 2355 Zanker Rd., San Jose, CA 95131-1138, USA.

[9] V.Katchorovski, J-Q. Lu, and M.S. Shur, "Broad Band Plasma Wave Detector Below Threshold Voltage in High Electron Mobility Transistors: Theory and Experiment", unpublished.

[10] T. A. Fjeldly, T. Ytterdal, and M. S. Shur, Introduction to Device Modeling and Circuit Simulation, John Wiley & Sons, New York, 1998.